



# Interacting tipping elements increase risk of climate domino effects under global warming

Nico Wunderling<sup>1,2,3</sup>, Jonathan F. Donges<sup>1,4</sup>, Jürgen Kurths<sup>1,5</sup>, and Ricarda Winkelmann<sup>1,2</sup>

<sup>1</sup>Earth System Analysis and Complexity Science, Potsdam Institute for Climate Impact, Research (PIK), Member of the Leibniz Association, 14473 Potsdam, Germany

<sup>2</sup>Institute of Physics and Astronomy, University of Potsdam, 14476 Potsdam, Germany

<sup>3</sup>Department of Physics, Humboldt University of Berlin, 12489 Berlin, Germany

<sup>4</sup>Stockholm Resilience Centre, Stockholm University, Stockholm, SE-10691, Sweden

<sup>5</sup>Saratov State University, Saratov, RU-410012, Russia

**Correspondence:** Nico Wunderling (nico.wunderling@pik-potsdam.de), Ricarda Winkelmann (ricarda.winkelmann@pik-potsdam.de)

**Abstract.** There exists a range of subsystems in the climate system exhibiting threshold behaviour which could be triggered under global warming within this century resulting in severe consequences for biosphere and human societies. While their individual tipping thresholds are fairly well understood, it is of yet unclear how their interactions might impact the overall stability of the Earth's climate system. This cannot be studied yet with state-of-the-art Earth system models due to computational constraints as well as missing and uncertain process representations of some tipping elements.

Here, we explicitly study the effects of known physical interactions between the Greenland and West Antarctic Ice Sheet, the Atlantic Meridional Overturning Circulation, the El-Niño Southern Oscillation and the Amazon rainforest using a conceptual network approach. We analyse the risk of domino effects being triggered by each of the individual tipping elements under global warming in equilibrium experiments, propagating uncertainties in critical temperature thresholds and interaction strengths via a Monte-Carlo approach.

Overall, we find that the interactions tend to destabilise the network. Furthermore, our analysis reveals the qualitative role of each of the five tipping elements showing that the polar ice sheets on Greenland and West Antarctica are oftentimes the initiators of tipping cascades, while the AMOC acts as a mediator, transmitting cascades.

This implies that the ice sheets, which are already at risk of transgressing their temperature thresholds within the Paris range of 1.5 to 2 °C, are of particular importance for the stability of the climate system as a whole.

## 1 Introduction

In the Earth system, there exists a range of large-scale subsystems, the so-called *tipping elements*. They can undergo sudden, qualitative and possibly irreversible changes in response to environmental perturbations once a certain critical threshold in forcing is exceeded (Lenton, 2008). Under such conditions, the actual tipping process might then take years up to millennia depending on the respective element separating critical forcing and realisation time of tipping (Hughes, 2013; Lenton, 2008). Among the tipping elements are cryosphere entities such as the continental ice sheets on Greenland and Antarctica, biosphere



components such as the Amazon rainforest or coral reefs as well as circulation patterns such as monsoon systems or the Atlantic Meridional Overturning Circulation. With continuing global warming, critical thresholds of some tipping elements might be exceeded within this century triggering severe consequences for the biosphere and human societies. These critical thresholds can be quantified with respect to the global mean temperature (GMT) resulting in three clusters of tipping elements that are characterised by their critical temperature (between 1-3 °C, 3-5 °C, above 5 °C respectively) (Schellnhuber, 2016). In the most vulnerable cluster from 1-3 °C above pre-industrial, there are mostly cryosphere entities such as the Greenland and West Antarctic Ice Sheet, the Arctic summer sea ice and mountain glaciers.

However, the tipping elements are not isolated systems but they interact on a global scale (Lenton, 2019; Kriegler, 2009). These interactions can have dampening or enhancing effects on the probability of tipping cascades and it remains an important issue to understand how this affects the overall stability of the Earth system. As of yet, current state-of-the-art global Earth system models cannot comprehensively simulate the nonlinear behaviour of many of the tipping elements due to uncertainties in process representations that would be relevant for modelling threshold behaviour as well as due to computational limitations, as for instance for the polar ice sheets. Furthermore, the interactions between tipping elements can also not yet be described in a framework of more simple process-based models in general since the interaction structure of tipping elements is not yet fully understood and partially explicitly based on expert knowledge.

In turn, for a subset of five tipping elements an expert elicitation was conducted synthesising a causal interaction structure and an estimation for the probability of cascading, nonlinear responses (Kriegler, 2009). These tipping elements are the Greenland Ice Sheet, the West Antarctic Ice Sheet, the Atlantic Meridional Overturning Circulation (AMOC), the El-Niño Southern Oscillation (ENSO) and the Amazon rainforest (see Fig. 1). Although this network might not be complete with respect to the physical interactions between the tipping elements and in the actual set of tipping elements themselves, it is a challenging approach to reveal dynamic interdependencies among a subset of tipping elements.

Observations from the last decades show that all five tipping elements are already impacted by progressing climate change (IPCC, 2014). The mass loss rate of Greenland and West Antarctica has increased and accelerated over the past decades (Shepherd, 2018; Khan, 2014; Zwally, 2011). Recent studies suggest that some parts, especially in the Amundsen basin in West Antarctica, might already have crossed a tipping point (Favier, 2014). The grounding lines of glaciers in this region are retreating rapidly, which could induce an instability mechanism (Marine Ice Sheet Instability) eventually leading to the disintegration of the whole region. Under unmitigated global warming, other parts of Antarctica are likely to follow, since they comply to the same dynamics and instabilities (Winkelmann, 2015). Also from paleo records, it is suggested that parts of Antarctica and larger parts of Greenland might already have experienced strong ice retreat in the past, especially during the Pliocene as well as in the Marine Isotope Stages 5e and 11 (Dutton, 2015).

It has also been shown that the AMOC experienced a significant slow-down since the mid of the last century (Caesar, 2018) potentially due to freshening of the Atlantic ocean by increased meltwater inflows from Greenland (Bakker, 2016; Böning, 2016). This trend and a bistability was also found in global circulation models and Earth system models of intermediate complexity (Drijfhout, 2012; Hawkins, 2011; Driesschaert, 2007; Jungclauss, 2006; Rahmstorf, 2005). Using proxies from sea surface, air temperatures and a global climate model, it has been observed that the AMOC slowed down significantly before



the beginning of the Holocene (Ritz, 2013).

The Amazon rainforest is not only directly impacted by anthropogenic climate change for instance through severe droughts or heat waves (Marengo, 2015; Brando, 2014), but also by deforestation and fire (Malhi, 2009). This increases the risk that parts  
60 of it will transit from a rainforest to a savanna state for instance through a diminished moisture recycling ratio (Staal, 2018; Zemp, 2017). It is suspected that the Amazon rainforest could be close to a critical deforestation ratio which might, together with global warming, suffice to start such a critical transition (Nobre, 2016). This could cause 30-50% of the forest to shift to tropical savanna or dry forests (Nobre, 2016). Tipping of ENSO implies a transition from chaotic occurrences on a multi-year basis to a steadification of major El-Niño events (Dekker, 2018; Cai, 2014). In simulations of CMIP3, CMIP5 and perturbed  
65 physics models, it was found that the frequency of El-Niño events can increase twofold in climate change scenarios (Taylor, 2012; Collins, 2010; Meehl, 2007).

## 2 Methods

### 2.1 Threshold effects and network modelling approach

70 For each of the five tipping elements investigated here, conceptual models exist that describe their basic dynamics. These conceptual models show distinct states of the tipping elements separated by a bifurcation, in most cases implying a hysteresis behaviour. In these conceptual approaches, tipping leads to an abrupt shift for instance from an “on” to an “off” (shutdown) state for the AMOC (Stommel, 1961), from ice-covered to essentially ice-free Greenland or West Antarctica (Levermann, 2016) and from a tree-covered state to a partial savanna or treeless state in the Amazon rainforest (Staal, 2015; Nes, 2014).

75 For ENSO, the threshold effect can be described by a Hopf-bifurcation, where a transition between a chaotic occurrence of El-Niño events and a more steady El-Niño has been suggested (Timmermann, 2003). The representation as a Hopf-bifurcation implies that no hysteresis occurs for ENSO. In first coupled experiments for AMOC and ENSO with these conceptual models, it was found that tipping of the AMOC makes it more likely for ENSO to undergo a critical transition as well (Dekker, 2018).

80 Based on these conceptual models as well as on first coupled experiments with a discrete state Boolean model (Gauchere, 2017), we here describe the interactions of the five tipping elements in a network approach using a set of coupled, topologically equivalent differential equations (Kuznetsov, 2004). This means that the main dynamics of each of the tipping elements are condensed to a non-linear differential equation with two stable states representing the current baseline state and a possible transitioned state capturing the qualitative dynamics of the respective tipping element (see Sect. 2.2, Eqs. 1 and 2).

85 Our conceptual approach makes use of these simplifications also because more comprehensive Earth system models cannot yet adequately represent tipping elements and more simple process-based models of tipping elements do not yet exist in a global network. As such, our aim is not to describe or model the related physical processes in much detail, but rather to investigate the risk of tipping cascades within the network. This is important since some tipping elements might already show

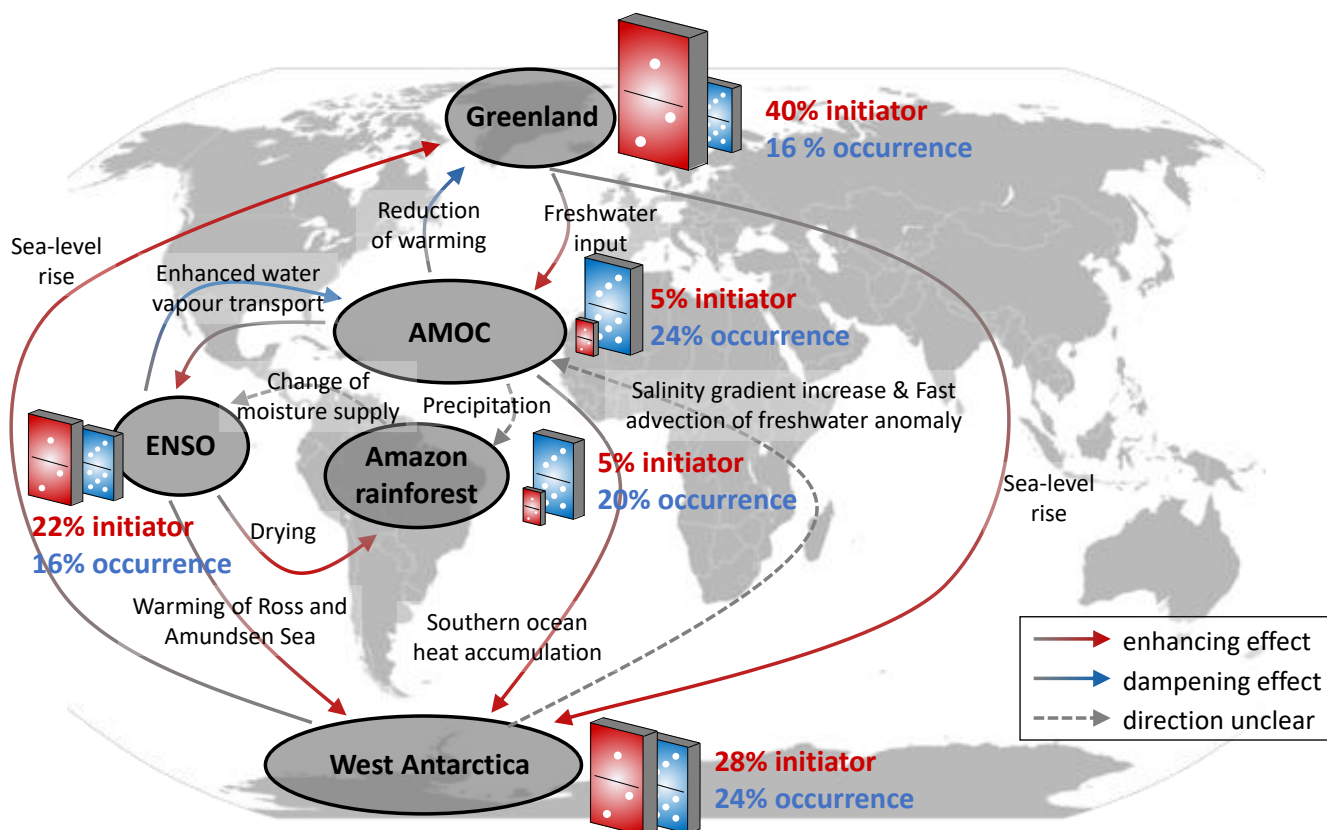


**Figure 1.** Interactions between climate tipping elements and their roles in tipping cascades. The Greenland Ice Sheet, West Antarctic Ice Sheet, Atlantic Meridional Overturning Circulation (AMOC), El-Niño Southern Oscillation (ENSO) and the Amazon rainforest are depicted together with their main interaction pathways (Kriegler, 2009). The interaction links between the tipping elements are colour-marked, where red arrows depict enhancing effects and blue arrows depict dampening effects. Where the direction is unclear, the link is marked in grey. A more thorough description of each of the tipping elements and the links can be found in Tables 1 and 2. Where tipping cascades arise, the relative size of the dominoes illustrates in how many model representations the respective climate components initiates (red domino) or is part of (blue domino) cascading transitions. Standard deviations for these values are given in Figs. S1(a) and (b). Generally, the polar ice sheets are found to more frequently take on the role as initiators than the equatorial tipping elements.



early warning signals of their beginning disintegration (Lenton, 2019; Favier, 2014). Consequently, the results of this study can  
 90 lay the foundations of a more detailed analysis with more complex models.

## 2.2 Differential equation model and physical interpretation of interactions

Each tipping element in the network is modeled by the non-linear differential equation

$$\frac{dx_i}{dt} = \left[ \underbrace{-x_i^3 + x_i + c_i}_{\text{Individual dynamics term}} + \underbrace{\frac{1}{2} \sum_{\substack{j \\ j \neq i}} d_{ij} (x_j + 1)}_{\text{Coupling term}} \right] \frac{1}{\tau_i}, \quad (1)$$

where  $x_i$  indicates the state of a certain tipping element,  $c_i$  is the critical parameter and  $\tau_i$  the typical tipping time scale with  $i =$   
 95 {Greenland Ice Sheet, West Antarctic Ice Sheet, AMOC, ENSO, Amazon rainforest}. This equation has been investigated in  
 different network types and widely been applied to systems in ecology, economics, political and medical frameworks (Krönke,  
 2019; Brummitt, 2015; Abraham, 1991). While the first term (*Individual dynamics term*) indicates the dynamical properties of  
 each tipping element, the second term (*Coupling term*) describes the connections of each tipping element to the other elements  
 (Fig. 1). If the prefactors in front of the cubic and the linear term are one and the additive coupling term is neglected, the critical  
 100 values where state changes occur are  $c_{i\ 1,2} = \pm\sqrt{4/27}$ . The differential equation is bistable for critical parameters between  
 $c_1$  and  $c_2$  and can here be separated into a *transitioned* and a *baseline* state, where  $x_i = -1$  denotes the baseline state and  
 $x_i = +1$  the completely transitioned one. The critical parameter  $c_i$  is modelled by the increase of the global mean temperature,  
 i.e.,  $c_i = \frac{\sqrt{4/27}}{T_{\text{limit},i}} \cdot \Delta\text{GMT}$ , where  $T_{\text{limit},i}$  is the critical temperature and  $\Delta\text{GMT}$  the increase of the global mean temperature.  
 This means that a state change occurs as soon as the increase of the GMT is higher than the critical temperature (see Table 1).

105

Tipping element	$\Delta T_{\text{limit}}$ (°C)
Greenland	0.8 – 3.2
West Antarctica	0.8 – 5.5
AMOC	3.5 – 6.0
ENSO	3.5 – 7.0
Amazon rainforest	3.5 – 4.5

**Table 1.** Nodes in the network of tipping elements. For each tipping element in the network (see Fig. 1) a range of critical temperatures  $\Delta T_{\text{limit}}$  is known from literature (Schellnhuber, 2016). In this temperature range, the tipping element is likely to undergo a transition.

In addition, we also model the physical interactions between the tipping elements as a linear coupling (first order approach). The coupling term  $\frac{1}{2} \sum_j d_{ij} (x_j + 1)$  consists of a sum of linear couplings to other elements  $x_j$  with  $d_{ij} = d \cdot s_{ij}/5$ . It is necessary to add +1 on top of  $x_j$  such that the direction (sign) of coupling is only determined by  $d_{ij}$  and not by the state  $x_j$ .



Thus, equation 1 becomes

$$110 \quad \frac{dx_i}{dt} = \left[ -x_i^3 + x_i + \frac{\sqrt{4/27}}{T_{\text{limit}, i}} \cdot \Delta\text{GMT} + \frac{d}{10} \cdot \sum_{\substack{j \\ j \neq i}} s_{ij} (x_j + 1) \right] \frac{1}{\tau_i}. \quad (2)$$

Here  $d$  is the *interaction strength* parameter that we vary in our simulations and  $s_{ij}$  is the link strength based on the expert elicitation (Kriegler, 2009) (see Table 2 & Sect. 2.5, *model initialisation and uncertainties*). There exists a physical process equivalent of the conceptual couplings behind each pair of tipping elements (see Table 2).

Note that we adapted the link from ENSO to AMOC from uncertain to negative since there is only a dampening process  
115 known in literature (Lenton, 2013). In this network of tipping elements, very strong connections exist, e.g., between Greenland and the AMOC. On the one hand side melting of Greenland enhances tipping of the AMOC via freshwater influx in the North Atlantic, while on the other hand a transitioned AMOC would hinder that warm water from the equator reaches Greenlandic regions thus cooling the ice sheet (see exemplary timelines Fig. 2(b)). The reason for a state transition is twofold, either through the increase of GMT or through the coupling to other tipping elements (Fig. 2(a)). Further important couplings are the impact  
120 of Greenland on West Antarctica via rising sea levels intensified by gravitational changes that are more pronounced on the Southern hemisphere if the gravitational power of Greenland is lost through disintegration of its ice sheet. Strong connections also exist in lower, equatorial latitudes between the ENSO and the Amazon rainforest, where a transitioned ENSO might significantly lower the precipitation over Amazonia.

125 The interaction strength  $d$  is described as a dimensionless constant of connection strength between the tipping elements (see Eq. 2). It is varied over a wide range in our simulations due to the uncertainties in the actual physical interaction strength between the tipping elements such that a variety of different scenarios can be investigated, i.e., for  $d \in [0; 1]$ . An interaction strength of 0 implies no coupling between the elements such that only the individual dynamics remain. If the interaction strength reaches high values around 1, the coupling term reaches the same magnitude as the individual dynamics term.

130

Summarized this means, if the critical temperature threshold of a tipping element is surpassed, it transgresses into the transitioned state and can potentially increase the likelihood of further tipping events via its interactions: for instance, the increased freshwater influx from Greenland Ice Sheet melt can induce a slow-down or even collapse of the AMOC (Fig. 2(b)). In our simulations, we consider increases of the global mean temperature from 0 up to 8 °C above pre-industrial, which could be  
135 reached in worst-case scenarios for the extended representative concentration pathway 8.5 (RCP 8.5) until 2500 (Schellnhuber, 2016; IPCC, 2014).

### 2.3 Time series and evaluation of tipping cascades

As long as the state of a certain tipping element is negative, we call this the *baseline* state. However, when the state variable of a tipping element crosses the limit of the lower grey hatched area within the course of a simulation run, a state transition occurs  
140 due to the global mean temperature and interactions between the respective tipping elements (see Figs. 2 and 3). The respective



Edge	Maximal link strength $s_{ij}$ (a.u.)	Physical process
Greenland → AMOC	+10	Freshwater inflow
AMOC → Greenland	-10	AMOC breakdown, Greenland cooling
Greenland → West Antarctica	+10	Grounding line retreat
ENSO → Amazon rainforest	+10	Drying over Amazonia
ENSO → West Antarctica	+5	Warming of Ross and Amundsen seas
AMOC → Amazon rainforest	$\pm 2$ up to $\pm 4$	Changes in hydrological cycle
West Antarctica → AMOC	$\pm 3$	Increase in meridional salinity gradient (-), Fast advection of freshwater anomaly to North Atlantic (+)
AMOC → ENSO	+2	Cooling of North-East tropical Pacific with thermo- cline shoaling and weakening of annual cycle in EEP
West Antarctica → Greenland	+2	Grounding line retreat
ENSO → AMOC	-2	Enhanced water vapour transport to Pacific
AMOC → West Antarctica	+1.5	Heat accumulation in Southern Ocean
Amazon rainforest → ENSO	$\pm 1.5$	Changes in tropical moisture supply

**Table 2.** Edges in the network of tipping elements. For each edge in the network of Fig. 1, there is a strength and a sign for each interaction of the tipping elements. The sign indicates if the interaction between the tipping elements is increasing or decreasing the danger of tipping cascades. After Kriegler et al. (2009) (Kriegler, 2009), the strength  $s_{ij}$  gives the index in terms of increased or decreased probability of cascading transitions. E.g., if Greenland transgresses its threshold, the probability that the AMOC does as well is increased by a factor of 10 (see entry for Greenland → AMOC). Then a random number between +1 and  $s_{ij} = s_{\text{Greenland} \rightarrow \text{AMOC}} = +10$  is drawn for our simulations. The other way round, the probability that Greenland transgresses its threshold in case the AMOC is in the transitioned state is decreased by a factor of  $\frac{1}{10}$ . Then a random number between -1 and  $s_{ij} = s_{\text{AMOC} \rightarrow \text{Greenland}} = -10$  is drawn. Furthermore, the main physical processes that connect pairs tipping elements are described in this table. The link strengths are grouped into strong, intermediate and weak links. Data and physical processes are taken from existing literature (Lenton, 2013; Kriegler, 2009).





tipping element then ends up in the upper hatched area and remains in the *transitioned* state. The time series for an in-depth example include temperature increases of 1.8, 1.9, 2.0 and 2.1 °C (columns) above pre-industrial and interaction strengths of 0.16, 0.32 and 0.48 (rows, see Fig. 3). From left to right panels, the global mean temperature is increased by 0.1 °C and hence a tipping cascade is initiated.

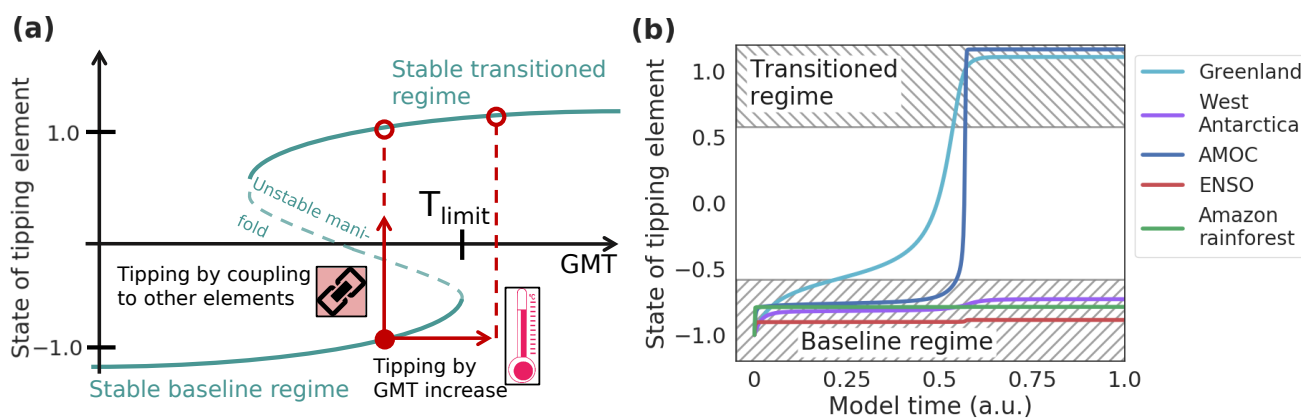


**Figure 2.** Schematic of generalised tipping element and time-series of tipping cascade. **(a)** Exemplary bifurcation diagram of a tipping element with two stable regimes: The lower state indicates the stable baseline regime, the upper state the stable transitioned regime. In case of the Greenland Ice Sheet, for instance, these correspond to its pre-industrial, almost completely ice-covered state (stable baseline regime) and an almost ice-free state (stable transitioned regime), as can be expected on the long-term for higher warming scenarios (Robinson, 2012). There are two ways how a tipping element can transgress its critical boundary (*unstable manifold*) and transition into the transitioned state, either by an increase of the global mean temperature or via interactions with other climate components. In both cases, the tipping element ends up in the stable transitioned regime indicated by the red full and hollow circles. **(b)** Exemplary time series showing a tipping cascade of two elements. Here, Greenland transgresses its critical temperature ( $T_{\text{limit, Greenland}}$ ) first, i.e., would become ice-free. Through its interaction with the AMOC (in particular, due to increased freshwater flux into the North Atlantic from the melting ice sheet), the AMOC then transgresses the unstable manifold in vertical direction (following the path of the red upward directed arrow in panel (a)). This example is based on a scenario with global mean temperature increase of 3.0 °C above pre-industrial levels and an interaction strength  $d$  of 0.10 (see methods in Chapt. 2).

145 In our example, the interaction strength determines the size of the tipping cascade, here from one to three (see Figs. 3(a), (b) and (c)). Still, the size, the timing and the occurrence of cascades also depend on the specific initial conditions. However, in general, the size of tipping cascades increases with higher interaction strengths and higher global warming. In these examples, we only show conditions where a tipping event takes place. This might not be the case for other conditions, e.g., lower global mean temperature increases, other couplings or other initial conditions. The initial conditions for the specific example of Fig. 3  
 150 can be found in supplementary Table S1.

We count tipping cascades as the difference in the number of transitioned elements at a steady interaction strength  $d$  with two slightly different global mean temperatures in the following way: we increase the GMT slightly (by 0.1 °C) between two



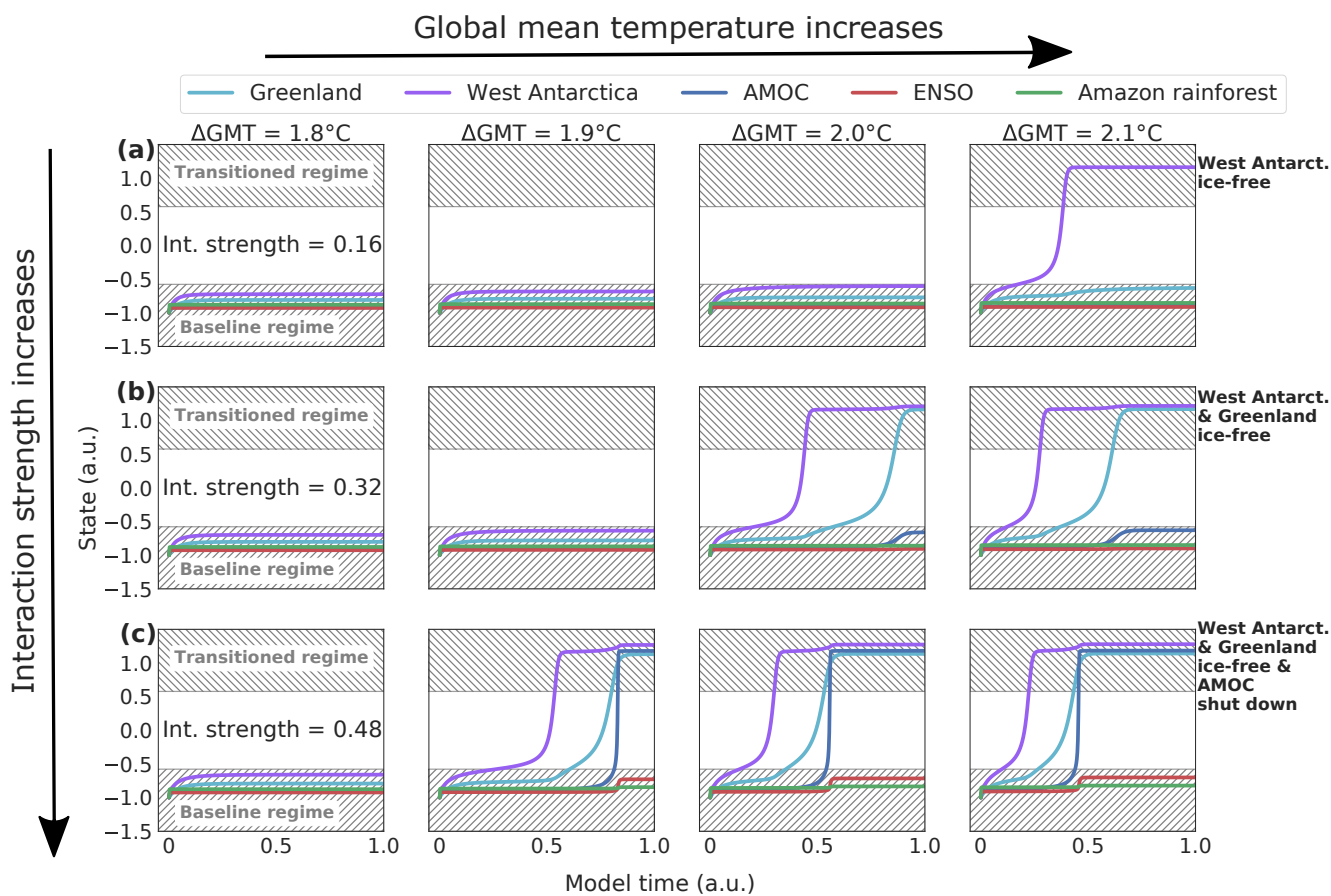


**Figure 3.** Time series of tipping cascades. Exemplary time series of states for each of the five investigated tipping elements, here simulated until equilibrium is reached. For comparability reasons, the initial conditions for the time series are the same (see Table S1) and all time series are computed for  $\Delta\text{GMT}$  increases of 1.8, 1.9, 2.0 and 2.1 °C above pre-industrial (columns). Couplings are constant for each row. Tipping cascades as shown here are defined as the number of transitioned elements at a fixed interaction strength and  $\Delta\text{GMT}$  compared to the simulation with a slightly higher  $\Delta\text{GMT}$  ( $\Delta\text{GMT}$  increase by 0.1 °C), but same interaction strength. If, between these two simulations, some of the tipping elements alter their equilibrium state, then a tipping cascade of the respective size occurred and is counted as such. **(a)** Singular tipping event for an interaction strength of 0.16. Tipping occurs at 2.1 °C. **(b)** Tipping cascade of size two for an interaction strength of 0.32. The cascade occurs at 2.0 °C. **(c)** Tipping cascade of size three for an interaction strength of 0.48, where tipping occurs at 1.9 °C. For other initial conditions, interaction strengths and global mean temperatures ( $\Delta\text{GMT}$ ) tipping cascades of size four and five can occur, too. Additionally, we marked the baseline and the transitioned regime as grey hatched areas. Between the hatched areas, the value of the time series is not stable and a critical state transition occurs. In the lower grey area, the element is called to be in the *baseline* regime and in the *transitioned* regime in the upper grey region.



subsequent equilibrium simulations. In case the number of transitioned elements differs between these two simulations, then a cascade of the respective size is counted at the GMT, where the state change occurred. Furthermore, the tipping element  
155 whose critical temperature threshold is closest to the temperature of tipping is counted as the tipping element which initiated this cascade.

## 2.4 Time scales

The five tipping elements in the coupled system of differential equations form a so-called *fast-slow system* (Kuehn, 2011) de-  
160 scribing a dynamical system with slowly varying parameters compared to fast changing states  $x_i$ . We calibrate typical tipping time scales by multiplying the right hand side of equation 1 with the inverse of the typical tipping time scale  $\tau_i$  such that a critical transition from the baseline to the transitioned state takes the adjusted amount of time in our model. Based on literature values for tipping times (Dekker, 2018; Winkelmann, 2015; Robinson, 2012; Lenton, 2008), we set the tipping time scale for the Greenland Ice Sheet, West Antarctic Ice Sheet, AMOC, ENSO and the Amazon rainforest to 4900, 2400, 300, 300 and 50  
165 years at 4 °C above pre-industrial. The tipping time scale is calibrated at this one point in the case of no interaction between the elements. After calibration, the tipping time is allowed to scale freely with changes in the GMT and the interaction strength  $d$ .

Since this model is a conceptual model and we are running equilibrium experiments only, we are only interested in the difference (and not the absolute value) between the tipping times as they can be decisive if a cascade emerges or not. The time  
170 each experiment is run is more than eight times the tipping time of the slowest tipping element which is until the equilibrium is reached in our experiments. In turn, the actual *absolute* number of the tipping time value is difficult to interpret and should not be taken as a prognosis of how long a potential tipping cascade takes. Therefore, the figures show model years in arbitrary units.

## 2.5 Model initialisation and uncertainties

175 Since the absolute strength of interactions between the tipping elements is highly uncertain, a dimensionless interaction strength is varied over a wide range in our network approach to cover a multitude of possible scenarios (see Chapt. 2 for detailed methods). To cope with the uncertainties in the critical temperatures and in the link strengths between pairs of tipping elements (see Eq. 2, Tables 1 and 2), we set up a Monte-Carlo ensemble with approximately 11 million members in total.

This Monte Carlo ensemble is set up as follows: we use a sample of 100 starting conditions of critical temperatures and link  
180 strengths  $s_{ij}$  from the uncertainty ranges given in literature (see Tables 1 and 2) (Schellnhuber, 2016; Kriegler, 2009). We model the uncertainty in the critical temperatures and the link strengths by drawing values randomly from a uniform distribution with a latin-hypercube algorithm (Baudin, 2013). Note that in the expert elicitation (Kriegler, 2009), there has been an estimation of the maximum increase or decrease of the tipping probability in case the element which starts the interaction is already in the transitioned state. For example, the link between Greenland and AMOC is given as [1; 10] in Kriegler et al. (2009) and  
185 is here modelled as a randomly drawn variable between 1 and 10 for  $s_{ij}$ . An example for an unclear coupling would be the



link between West Antarctica and AMOC which is given as [0.3; 3] in Kriegler et al. (2009) which we translate into an  $s_{ij}$  between  $-3$  and  $3$ . In general, the values are drawn between  $1$  and the respective maximum value  $s_{ij}$  if the connection between  $i$  and  $j$  is positive or between  $-1$  and the negative maximum value  $s_{ij}$  if the connection between  $i$  and  $j$  is negative (see Table 2). Since our model has 17 parameters with uncertainties, we use a latin-hypercube sampling to construct a set of starting  
190 conditions for the Monte Carlo simulation such that the space of starting conditions is covered better than with a usual random sample generation (Baudin, 2013). With this set of 100 starting conditions, we simulate the state for each pair of global mean temperatures and interaction strengths  $d$ .

We also simulate all 27 different network types which arise when we permute all possibilities (negative, zero, positive) from the three unclear links AMOC  $\rightarrow$  Amazon rainforest, West Antarctica  $\rightarrow$  AMOC and Amazon rainforest  $\rightarrow$  ENSO (see Table 2  
195 and Fig. 1). For each of these 27 network types, we compute the same 100 starting conditions that we received from our latin-hypercube sampling. Thus, in total, we compute 2700 samples for each GMT ( $0.0 - 8.0$  °C, step width:  $0.1$  °C) and interaction strength ( $0.0 - 1.0$ , step width:  $0.02$ ) ending up a large ensemble of 11 million members overall.

### 3 Results

#### 3.1 Critical temperature ranges

200 For each individual tipping element, global mean temperature thresholds have been identified (Schellnhuber, 2016), showing that Greenland and West Antarctica might already be at risk within the Paris range while AMOC, ENSO and the Amazon rainforest have a higher critical temperature range (Fig. 4(a)). Assuming a uniform distribution, we draw random values from these individual temperature ranges as initial conditions for our Monte-Carlo ensemble.

Owing to the interactions between the tipping elements, the critical temperatures are generally shifted to lower values  
205 (Figs. 4(b) and (c)). This lowering of the temperature thresholds is almost linear for the Amazon rainforest and ENSO with increasing interaction strength, while for West Antarctica and AMOC, we find a sharp decline for interaction strengths up to  $0.2$  and an approximately constant critical temperature range afterwards.

In particular, the mean critical temperature for these four tipping elements is lowered by about  $1.4$  °C (45%) for West Antarctica,  $2.75$  °C (55%) for AMOC,  $2.75$  °C (50%) for ENSO and  $2.1$  °C (55%) the Amazon rainforest, respectively (Fig. 5).  
210 This is likely due to the predominantly positive links between these tipping elements (see Fig. 1).

In contrast, the critical temperature range for the Greenland Ice Sheet can in fact be raised due to the interaction with the other tipping elements, accompanied by increasing uncertainty. This can be explained by the strong positive-negative interaction loop between Greenland and the AMOC (see Table 2): On the one hand, enhanced meltwater influx into the North Atlantic might dampen the AMOC (positive feedback), while on the other hand, a weakened overturning circulation would lead to a net-  
215 cooling effect around Greenland (negative feedback). Thus, the state of Greenland strongly depends on the specific initial conditions in critical temperature and interaction strength of the respective Monte-Carlo ensemble member.

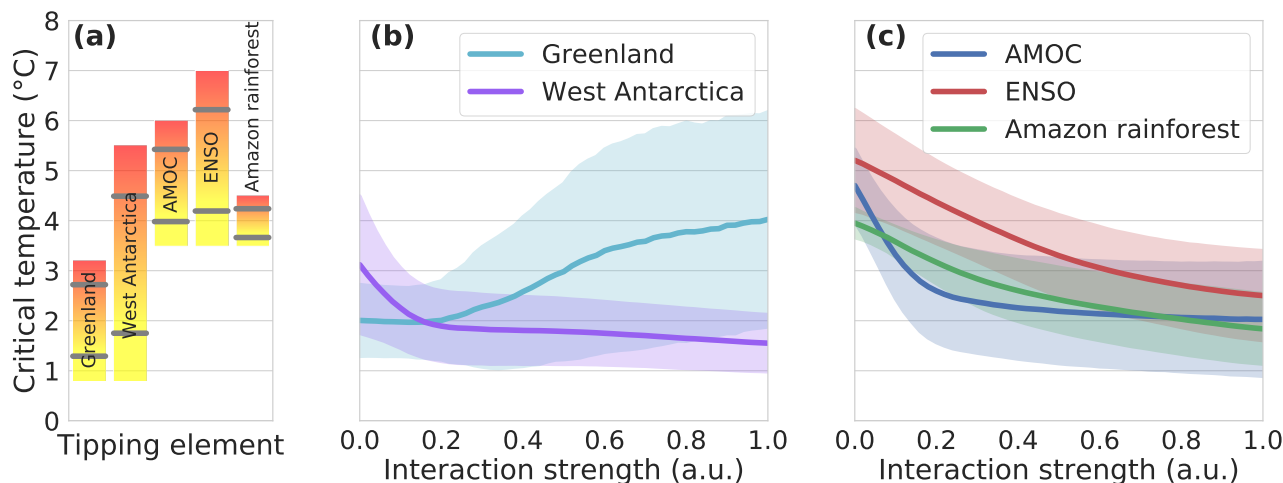


**Figure 4.** Shift of critical temperature ranges due to interactions. **(a)** Critical global mean temperatures for each of the five investigated tipping elements, without taking interactions into account (as reproduced from literature (Schellnhuber, 2016)). The grey bars indicate the standard deviation arising when drawing from a random uniform distribution between the respective upper and lower temperature limits. These bars correspond to the critical temperature ranges in case of zero interaction strength in panels **(b)** and **(c)**. **(b, c)** Change of critical temperature ranges with increasing interaction strength for the Greenland Ice Sheet and West Antarctic Ice Sheet (panel **(b)**) and the Atlantic Meridional Overturning Circulation (AMOC), El-Niño Southern Oscillation (ENSO) and Amazon rainforest (panel **(c)**). The standard deviation of the critical temperatures for each tipping element within the Monte Carlo ensemble is given as respective colour shading.

### 3.2 Risk of tipping cascades

Tipping cascades occur when two or more tipping elements transgress their critical thresholds for a given temperature level (see Sect. 2.3: *time series and evaluation of tipping cascades*). We evaluate the associated risk as the number of ensemble  
 220 representations in which such tipping cascades are detected. For global warming up to 2.0 °C, tipping occurs in 63% of all simulations (Fig. 6(a)). This comprises the tipping of individual elements (23%) as well as cascades including 2 elements  
 225 (15%), 3 elements (13%), 4 elements (10%) and all 5 elements (3%; see Fig. 6(b)).

Since the coupling between the tipping elements is highly uncertain, we introduce an upper limit of the maximum interaction strength and vary it from 0.0 to 1.0 (see Table 3). The highest value of 1.0 implies that the interaction between the elements is as  
 225 important as the nonlinear threshold behaviour of an individual element. For lower values, the interaction plays a less dominant role. We find that the occurrence of tipping events does not depend significantly on the maximum interaction strength - however, the cascade size decreases for lower values.

Tipping cascades are first induced at warming levels around 1 °C above pre-industrial, where the lower critical temperature threshold of the Greenland Ice Sheet is exceeded. The bulk of tipping cascades, however, is found between 1 and 3 °C GMT  
 230 increase. This is true for all cascade sizes (see Figs. 6(c, d) and Figs. S2(a, b)).

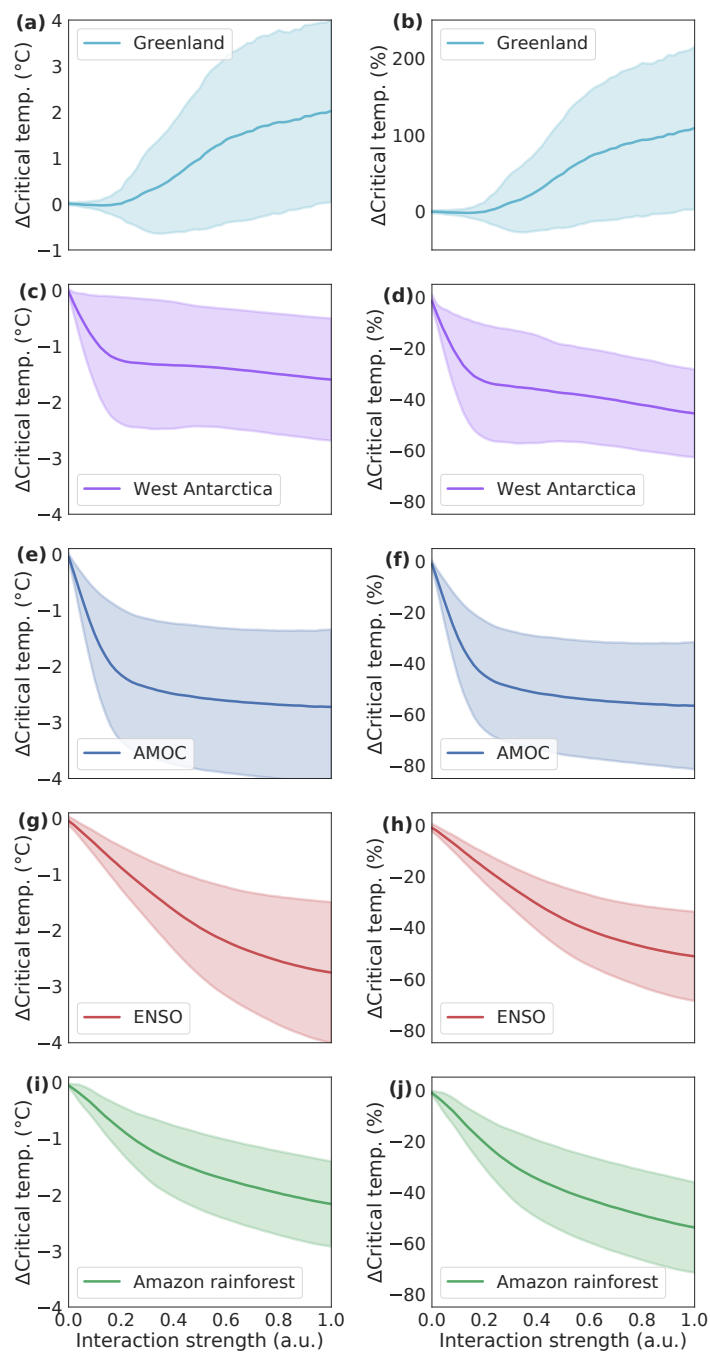


**Figure 5.** Difference in critical temperatures with respect to the interaction strength. Difference of critical temperatures in °C (left panels) and % (right panels) compared to the respective initially drawn critical temperature for the five investigated tipping elements: (a, b) Greenland Ice Sheet, (c, d) West Antarctic Ice Sheet, (e, f) AMOC, (g, h) ENSO and (i, j) Amazon rainforest. The standard deviation from the ensemble members is shown as respective colour shading.



Maximum interaction strength $d$	No tipping (%)	Tipping (%)	Cascade sizes (%)				
			1	2	3	4	5
1.0	37	63	23	15	13	10	3
0.75	39	61	27	14	12	7	1
0.50	40	60	33	13	11	4	0
0.25	40	60	45	12	4	0	0
0.10	41	59	55	4	0	0	0

**Table 3.** Fraction of tipping events. For different maximum values of the interaction strength  $d$  (first column), the fraction of networks is shown that have a tipping event or cascade (third column) within the Paris limit until the global mean temperature increase reaches 2.0 °C above pre-industrial. This means that 63% of all networks possess a tipping event or cascade, while 37% do not (second column) if all interaction strengths until 1.0 are considered (see Figs. 6(a, b)). Overall, the fraction of tipping events rather stays the same and only slightly goes down for lower limits of maximum interaction strengths. However, the distribution of tipping events and cascade sizes changes, i.e., the number of large cascade sizes decrease with lower limits of interaction strengths. This is shown in the last column that is split up between the percentage of cascades of size one, two, three, four and five.

For temperatures above 3 °C GMT increase, cascades occur less frequently since most of the tipping elements already transgress their threshold before this temperature is reached.

This analysis reveals that the five tipping elements can be grouped into two clusters, one comprising Greenland, West Antarctica and the AMOC, the other ENSO and the Amazon rainforest. The latter cluster is shifted towards higher temperature thresholds, where tipping cascades can still be triggered above 3.0 °C (Fig. S1(c)).

The most prevalent tipping pairs, as simulated in our network approach, consist of cascading transitions between the ice sheets and/or the AMOC, summing up to 60% of all tipping pairs (Fig. 6(e)), which supports the hypothesis of a polar ice-ocean and an equatorial ENSO-Amazon cluster.

While ENSO together with the Amazon rainforest makes for 30% of the tipping pairs due to their strong interlinkage via changes in moisture supply that exist in all network representations (compare Fig. 1 and Table 2), its role in tipping triplets is much smaller, with the most frequent combination together with AMOC and the Amazon around 15% (Fig. 6(f)).

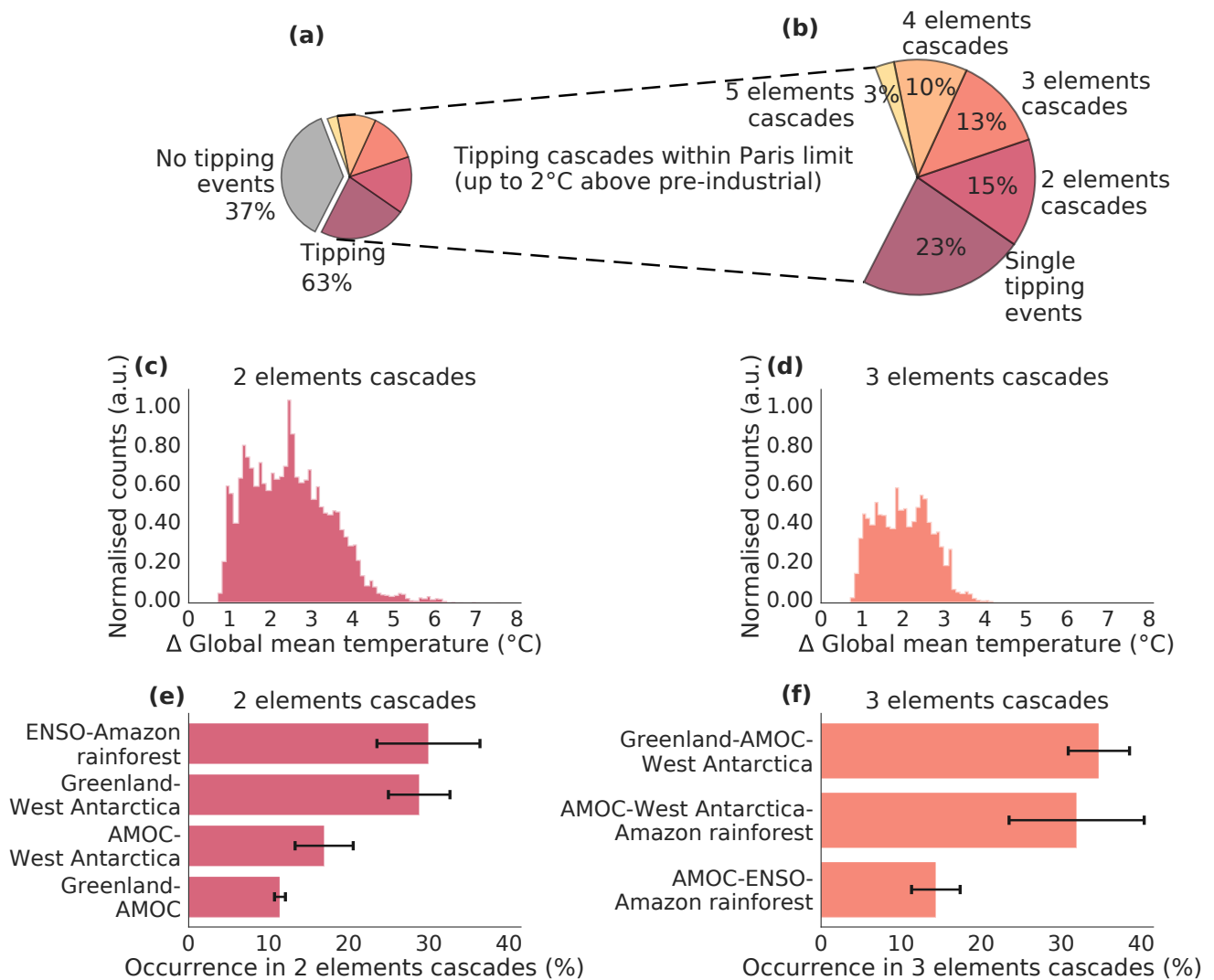


**Figure 6.** Tipping cascades. **(a, b)** For global warming up to 2.0 °C above pre-industrial, the colour shading illustrates the fraction of model representations in the Monte-Carlo ensemble without tipping events (grey), with a singular tipping event (purple) and with cascades including two (red), three (dark orange), four (orange) and five (yellow) elements. **(c, d)** Occurrence of tipping cascades of size two and three versus global mean temperature increase. The counts are normalised to the highest value of the most frequent tipping cascade (in cascades of size two). Tipping cascades of size three, four and five (Figs. S2(a, b)) are set to the same scale to secure comparability. **(e)**, Dominant cascades of size two for temperature increases from 0 – 8 °C above pre-industrial. **(f)**, Dominant cascades of size three for temperature increases from 0 – 8 °C above pre-industrial. Other cascades are not shown, since their relative occurrence is comparably much smaller. The standard deviation represents the difference between the network settings (see Sect. 2.2: *model initialisation and uncertainty*). It is larger for network representations where unclear links are involved, e.g., for the ENSO-Amazon rainforest tipping pair (compare Fig. 1 and Table 2).





### 3.3 Different roles of tipping elements

For each of the five tipping elements, we systematically assess their role within the climate network, generally distinguishing between initiators (triggering a cascade), followers (last element in a tipping chain) and mediators (elements in-between).

245 We find that in up to 40% of cases, the Greenland Ice Sheet appears to trigger tipping cascades. At the same time, it is among the elements which occur least frequently in cascades (around 16% of all cases, see Fig. 1). Thus, we call Greenland a *dominant initiator* of cascades.

Following this argument for Greenland, the West Antarctic Ice Sheet is both an *initiator* and *mediator* of cascades, since it occurs more often in cascades (24%) compared to other tipping elements and, likewise, often acts as the initiator (28%).

250 Although the frequency of occurrence and initiation of cascades is very similar for the AMOC and Amazon rainforest, their role can be clearly distinguished via the network structure. While the AMOC is a *dominant mediator* of cascades, the Amazon rainforest mainly is a *follower*. The Amazon rainforest follows critical transitions of other tipping elements out of two reasons: First, its critical temperature is small (3.5–4.5 °C) which makes it vulnerable to be drawn over its critical threshold by other elements.

255 Second, as argued above, it is strongly influenced by ENSO through the changes in moisture supply (Fig. 1). Keeping this in mind, the role of ENSO can be described as in-between mediator and initiator. Apart from the Amazon rainforest, other elements are far less influenced by ENSO. This can be observed when looking at the most frequent tipping cascade of size two and at temperatures above 3 °C (Fig. 6(e)), which almost exclusively consist of cascades between ENSO and the Amazon rainforest, which in turn are almost only triggered by ENSO at this temperature range (Fig. S1(c, d)).



#### 260 4 Conclusion and Discussion

It has been shown in previous studies that all of the five integral components of the Earth's climate system considered here, are at risk of transgressing into undesired states when critical thresholds are crossed (Schellnhuber, 2016; Lenton, 2008) and some of them have already been proposed as examples where a starting transition might be observable (Lenton, 2019). This may affect the stability of the current climate even in intermediate climate change scenarios consistent with the Paris Agree-  
265 ment (Steffen, 2018).

Here, we show that this risk increases significantly when considering interactions between these climate tipping elements. Altogether, with the exception of the Greenland Ice Sheet, interactions effectively push the critical threshold temperatures to lower warming levels, thus reducing the overall stability of the climate system. The domino-like interactions also foster cas-  
270 cading, nonlinear responses. Under these circumstances, our model indicates that the climate system generally decomposes into a polar and an equatorial tipping cluster. Cascades are predominantly initiated by the polar ice sheets and mediated by the AMOC. This also implies that the negative feedback loop between Greenland and the AMOC might possibly not be able to stabilise the climate system, a possibility that was raised in earlier work using a binary model approach (Gauchere, 2017).

275 While our conceptual model evidently does not resemble the full complexity of the Earth system and is not intended to simulate the multitude of physical processes, it allows us to systematically assess the qualitative role of the different interactions of some of the most important sub-regions of the climate system. The large-scale Monte Carlo approach further enables us to estimate the uncertainties associated with the interaction strengths, interaction directions and the individual temperature thresholds.

280 This work could form the basis for a more detailed investigation with Earth system models which can represent the full dynamics of each tipping element, but where computational constraints yet prohibit such a detailed analysis as presented here. In particular, the time-scales for potential tipping need to be rigorously explored in contrast to the conceptual usage of these terms here, considering that these might only manifest over multiple centuries or even millennia, as for instance for the continental ice sheets (Winkelmann, 2015; Lenton, 2008).



285 *Code and data availability.* The data that support the findings of this study are available from the corresponding author upon reasonable request. The code and the python software package “pycascades” that support the findings of this study are available from the corresponding author.

*Author contributions.* R.W., J.F.D. and N.W. designed the study. N.W. conducted the model simulation runs and prepared the figures. All authors discussed the results and wrote the manuscript.

290 *Competing interests.* The authors declare no competing interests.

*Acknowledgements.* This work has been carried out within the framework of the IRTG 1740/TRP 2015/50122-0 funded by DFG and FAPESP. N.W., J.K. and R.W. acknowledge their support. N.W. is grateful for a scholarship from the Studienstiftung des Deutschen Volkes. J.F.D. is grateful for financial support by the Stordalen Foundation via the Planetary Boundary Research Network (PB.net), the Earth League’s EarthDoc program, and the European Research Council Advanced Grant project ERA (Earth Resilience in the Anthropocene). R.W. acknowledges support by the European Union’s Horizon 2020 research and innovation programme under grant agreement no. 820575 (TiPACCs). We are thankful for support by the Leibniz Association project DominoES. The authors gratefully acknowledge the European Regional Development Fund (ERDF), the German Federal Ministry of Education and Research and the Land Brandenburg for supporting this project by providing resources on the high performance computer system at the Potsdam Institute for Climate Impact Research. Furthermore, we are thankful to Jobst Heitzig, Marc Wiedermann and Julius Garbe for discussions on this project as well as to Jonathan Krönke for support with the software package “pycascades”.

295  
300



## References

- Abraham, R., Keith, A., Koebbe, M., and Mayer-Kress, G.: Computational Unfolding Of Double-Cusp Models Of Opinion Formation, *Int. J. Bifurcat. Chaos*, 01, 417–430, 1991.
- 305 Bakker, P., Schmittner, A., Lenaerts, J.T.M., Abe-Ouchi, A., Bi, D., van den Broeke, M.R., Chan, W.L., Hu, A., Beadling, R.L., Marsland, S.J. and Mernild, S.H.: Fate of the Atlantic Meridional Overturning Circulation: Strong decline under continued warming and Greenland melting, *Geophysical Research Letters*, 43, 2016.
- Baudin, M.: pyDOE: The experimental design package for python, software available under the BSD license (3-Clause) at <https://pythonhosted.org/pyDOE/index.html>, 2013.
- 310 Böning, C. W., Behrens, E., Biastoch, A., Getzlaff, K., and Bamber, J. L.: Emerging impact of Greenland meltwater on deepwater formation in the North Atlantic Ocean, *Nat. Geosci.*, 9, 523–527, 2016.
- Brando, P.M., Balch, J.K., Nepstad, D.C., Morton, D.C., Putz, F.E., Coe, M.T., Silvério, D., Macedo, M.N., Davidson, E.A., Nóbrega, C.C., and Alencar, A.: Abrupt increases in Amazonian tree mortality due to drought-fire interactions, *P. Natl. Acad. Sci. USA*, 111, 6347–6352, 2014.
- 315 Brummitt, C. D., Barnett, G., and Dsouza, R. M.: Coupled catastrophes: sudden shifts cascade and hop among interdependent systems, *J. R. Soc. Interface*, 12, 439 20150712, 2015.
- Caesar, L., Rahmstorf, S., Robinson, A., Feulner, G., and Saba, V.: Observed fingerprint of a weakening Atlantic Ocean overturning circulation, *Nature*, 556, 191–196, 2018.
- Cai, W., Borlace, S., Lengaigne, M., Van Rensch, P., Collins, M., Vecchi, G., Timmermann, A., Santoso, A., McPhaden, M.J., Wu, L., and  
320 England, M.H.: Increasing frequency of extreme El Niño events due to greenhouse warming, *Nat. Clim. Change*, 4, 111–116, 2014.
- Collins, M., Booth, B.B., Bhaskaran, B., Harris, G.R., Murphy, J.M., Sexton, D.M., and Webb, M.J.: Climate model errors, feedbacks and forcings: a comparison of perturbed physics and multi-model ensembles, *Clim. Dynam.*, 36, 1737–1766, 2010.
- Dekker, M. M., Heydt, A. S. V. D., and Dijkstra, H. A.: Cascading transitions in the climate system, *Earth Syst. Dynam.*, 9, 1243–1260, 2018.
- 325 Driesschaert, E., Fichefet, T., Goosse, H., Huybrechts, P., Janssens, I., Mouchet, A., Munhoven, G., Brovkin, V., and Weber, S.L.: Modeling the influence of Greenland ice sheet melting on the Atlantic meridional overturning circulation during the next millennia, *Geophys. Res. Lett.*, 34, 2007.
- Drijfhout, S., Oldenborgh, G. J. V., and Cimatoribus, A.: Is a Decline of AMOC Causing the Warming Hole above the North Atlantic in Observed and Modeled Warming Patterns? *J. Climate*, 25, 8373–8379, 2012.
- 330 Dutton, A., Carlson, A.E., Long, A., Milne, G.A., Clark, P.U., DeConto, R., Horton, B.P., Rahmstorf, S. and Raymo, M.E.: Sea-level rise due to polar ice-sheet mass loss during past warm periods, *Science*, 349, aaa4019–aaa4019, 2015.
- Favier, L., Durand, G., Cornford, S.L., Gudmundsson, G.H., Gagliardini, O., Gillet-Chaulet, F., Zwinger, T., Payne, A.J. and Le Brocq, A.M.: Retreat of Pine Island Glacier controlled by marine ice-sheet instability, *Nat. Clim. Change*, 4, 117–121, 2014.
- Gaucherel, C. and Moron, V.: Potential stabilizing points to mitigate tipping point interactions in Earths climate, *Int. J. Climatol.*, 37, 399–408,  
335 2016.
- Hawkins, E., Smith, R.S., Allison, L.C., Gregory, J.M., Woollings, T.J., Pohlmann, H., and De Cuevas, B.: Bistability of the Atlantic overturning circulation in a global climate model and links to ocean freshwater transport, *Geophys. Res. Lett.*, 38, 2011.



- Hughes, T., Carpenter, S., Rockström, J., Scheffer, M., and Walker, B.: Multiscale regime shifts and planetary boundaries. *Trends Ecol. Evol.*, 28, 389–395, 2013.
- 340 IPCC: Stocker, T.F., Qin, D., Plattner, G.K., Tignor, M., Allen, S.K., Boschung, J., Nauels, A., Xia, Y., Bex, V. and Midgley, P.M.: Climate change 2013: the physical science basis: Working Group I contribution to the fifth assessment report of the intergovernmental panel on climate change, Cambridge University Press, 2014.
- IPCC Special Report: Global Warming of 1.5 °C – an IPCC special report on the impacts of global warming of 1.5 °C above pre-industrial levels and related global greenhouse gas emission pathways, in the context of strengthening the global response to the threat of climate change, sustainable development, and efforts to eradicate poverty, 2018.
- 345 Jungclaus, J. H., Haak, H., Esch, M., Roeckner, E., and Marotzke, J.: Will Greenland melting halt the thermohaline circulation? *Geophys. Res. Lett.*, 33, 17, 2006.
- Khan, S.A., Kjær, K.H., Bevis, M., Bamber, J.L., Wahr, J., Kjeldsen, K.K., Bjørk, A.A., Korsgaard, N.J., Stearns, L.A., Van Den Broeke, M.R., and Liu, L.: Sustained mass loss of the northeast Greenland ice sheet triggered by regional warming. *Nat. Clim. Change*, 4, 292–299, 350 2014.
- Kriegler, E., Hall, J.W., Held, H., Dawson, R., and Schellnhuber, H. J.: Imprecise probability assessment of tipping points in the climate system. *P. Natl. Acad. Sci. USA*, 106, 5041–5046, 2009.
- Krönke, J., Wunderling, N., Winkelmann, R., Staal, A., Stumpf, B., Tuinenburg, O.A., and Donges, J.F.: Dynamics of Tipping Cascades on Complex Networks, Preprint at <https://arxiv.org/abs/1905.05476>, 2019.
- 355 Kuehn, C. A mathematical framework for critical transitions: Bifurcations, fast–slow systems and stochastic dynamics, *Physica D*, 240, 1020–1035, 2011.
- Kuznetsov, Y. A.: *Elements of Applied Bifurcation Theory*, Applied Mathematical Sciences, Springer, New York, USA, doi:10.1007/978-1-4757-3978-7, 2004.
- Lenton, T. M., Held, H., Kriegler, E., Hall, J. W., Lucht, W., Rahmstorf, S., and Schellnhuber, H. J.: Tipping elements in the Earth's climate system. *P. Natl. Acad. Sci. USA*, 105, 1786–1793, 2008.
- 360 Lenton, T. M., and Williams, H. T.: On the origin of planetary-scale tipping points, *Trends Ecol. Evol.*, 28, 380–382, 2013.
- Lenton, T. M., Rockström, J., Gaffney, O., Rahmstorf, S., Richardson, K., Steffen, W., and Schellnhuber, H. J.: Climate tipping points — too risky to bet against. *Nature*, 575, 592–595, 2019.
- Levermann, A., and Winkelmann, R.: A simple equation for the melt elevation feedback of ice sheets, *The Cryosphere*, 10, 1799–1807, 2016.
- 365 Malhi, Y., Aragão, L.E., Galbraith, D., Huntingford, C., Fisher, R., Zelazowski, P., Sitch, S., McSweeney, C., and Meir, P.: Exploring the likelihood and mechanism of a climate-change-induced dieback of the Amazon rainforest, *P. Natl. Acad. Sci. USA*, 106, 20610–20615, 2009.
- Marengo, J. A., and Espinoza, J. C.: Extreme seasonal droughts and floods in Amazonia: causes, trends and impacts. *Int. J. Climatol.*, 36, 1033–1050, 2015.
- 370 Meehl, G.A., Covey, C., Delworth, T., Latif, M., McAvaney, B., Mitchell, J.F., Stouffer, R.J. and Taylor, K.E.: THE WCRP CMIP3 Multi-model Dataset: A New Era in Climate Change Research, *B. Am. Meteorol. Soc.*, 88, 1383–1394, 2007.
- Nes, E. H. V., Hirota, M., Holmgren, M., and Scheffer, M.: Tipping points in tropical tree cover: linking theory to data, *Glob. Change Biol.*, 20, 1016–1021, 2014.
- Nobre, C.A., Sampaio, G., Borma, L.S., Castilla-Rubio, J.C., Silva, J.S., and Cardoso, M.: Land-use and climate change risks in the Amazon and the need of a novel sustainable development paradigm, *P. Natl. Acad. Sci.*, 113, 10759–10768, 2016.
- 375



- Rahmstorf, S., Crucifix, M., Ganopolski, A., Goosse, H., Kamenkovich, I., Knutti, R., Lohmann, G., Marsh, R., Mysak, L.A., Wang, Z., and Weaver, A.J.: Thermohaline circulation hysteresis: A model intercomparison, *Geophys. Res. Lett.*, 32, 2005.
- Ritz, S., Stocker, T., Grimalt, J., Meniel, L., and Timmermann, A.: Estimated strength of the Atlantic overturning circulation during the last deglaciation, *Nat. Geosci.*, 6, 208–212, 2013.
- 380 Robinson, A., Calov, R., and Ganopolski, A.: Multistability and critical thresholds of the Greenland ice sheet, *Nat. Clim. Change*, 2, 429–432, 2012.
- Schellnhuber, H., Rahmstorf, S., and Winkelmann, R.: Why the right climate target was agreed in Paris. *Nat. Clim. Change*, 6, 649–653, 2016.
- Shepherd, A., Ivins, E., Rignot, E., Smith, B., Van Den Broeke, M., Velicogna, I., Whitehouse, P., Briggs, K., Joughin, I., Krinner, G., and  
385 Nowicki, S.: Mass balance of the Antarctic Ice Sheet from 1992 to 2017. *Nature*, 558, 219–222, 2018.
- Staal, A., Dekker, S. C., Hirota, M., and Nes, E. H. V.: Synergistic effects of drought and deforestation on the resilience of the south-eastern Amazon rainforest, *Ecol. Complex.*, 22, 65–75, 2015
- Staal, A., Tuinenburg, O.A., Bosmans, J.H., Holmgren, M., van Nes, E.H., Scheffer, M., Zemp, D.C., and Dekker, S.C.: Forest-rainfall cascades buffer against drought across the Amazon, *Nat. Clim. Change*, 8, 539–543, 2018.
- 390 Steffen, W., Rockström, J., Richardson, K., Lenton, T.M., Folke, C., Liverman, D., Summerhayes, C.P., Barnosky, A.D., Cornell, S.E., Crucifix, M., Donges, J.F., Fetzer, I., Lade, S.J., Scheffer, M., Winkelmann, R., and Schellnhuber, H.J.: Trajectories of the Earth System in the Anthropocene, *P. Natl. Acad. Sci. USA*, p.201810141, 2018.
- Stommel, H.: Thermohaline Convection with Two Stable Regimes of Flow, *Tellus*, 13, 224–230, 1961.
- Taylor, K. E., Stouffer, R. J., and Meehl, G. A.: An Overview of CMIP5 and the Experiment Design, *B. Am. Meteorol. Soc.*, 93, 485–498,  
395 2012.
- Timmermann, A., Jin, F.-F., and Abshagen, J.: A Nonlinear Theory for El Niño Bursting, *J. Atmos. Sci.*, 60, 152–165, 2003.
- Winkelmann, R., Levermann, A., Ridgwell, A., and Caldeira, K.: Combustion of available fossil fuel resources sufficient to eliminate the Antarctic Ice Sheet, *Science Advances*, 1, 2015.
- Zemp, D.C., Schleussner, C.F., Barbosa, H.M., Hirota, M., Montade, V., Sampaio, G., Staal, A., Wang-Erlandsson, L. and Rammig, A.:  
400 Self-amplified Amazon forest loss due to vegetation-atmosphere feedbacks, *Nat. Commun.*, 8, 14681, 2017.
- Zwally, H.J., Li, J., Brenner, A.C., Beckley, M., Cornejo, H.G., DiMarzio, J., Giovinetto, M.B., Neumann, T.A., Robbins, J., Saba, J.L., and Yi, D.: Greenland ice sheet mass balance: distribution of increased mass loss with climate warming: 2003–07 versus 1992–2002. *J. Glaciol.*, 57, 88–102, 2011.